bioRxiv preprint doi: https://doi.org/10.1101/494716; this version posted December 13, 2018. The copyright holder for this preprint (which was not certified by peer review) is the author/funder, who has granted bioRxiv a license to display the preprint in perpetuity. It is made available under aCC-BY 4.0 International license.

Cheater-mediated evolution shifts phenotypic heterogeneity in *Bacillus subtilis* biofilms

Marivic Martin[1,2], Anna Dragoš[1], Daniel Schäfer[2], Gergely Maróti[3], and Ákos T. Kovács[1,2]

[1] Bacterial Interactions and Evolution Group, Technical University of Denmark, 2800 Kongens Lyngby, Denmark

[2] Terrestrial Biofilms Group, Friedrich Schiller University Jena, 07743 Jena, Germany

[3] Institute of Plant Biology, Biological Research Center of the Hungarian Academy of Sciences, 3600 Szeged, Hungary

Corresponding Author: Ákos T. Kovács

Bacterial Interactions and Evolution Group, Technical University of Denmark, 2800 Kongens Lyngby, Denmark; atkovacs@dtu.dk; +45 45252527

Keywords: *Bacillus subtilis*, biofilm, phenotypic heterogeneity, experimental evolution, exopolysaccharide

bioRxiv preprint doi: https://doi.org/10.1101/494716; this version posted December 13, 2018. The copyright holder for this preprint (which was not certified by peer review) is the author/funder, who has granted bioRxiv a license to display the preprint in perpetuity. It is made available under aCC-BY 4.0 International license.

ABSTRACT

Biofilms are closely packed cells held and shielded by extracellular matrix composed of structural proteins and exopolysaccharides (EPS). As matrix components are costly to produce and shared within the population, EPS-deficient cells can act as cheaters by gaining benefits from the cooperative nature of EPS producers. Remarkably, genetically programmed EPS producers can also exhibit phenotypic heterogeneity at single cell level. For instance, mature biofilms of *Bacillus subtilis* contain cells in an 'ON' state, expressing extracellular matrix genes, as well as cells in an 'OFF' state. Previous studies have shown that spatial structure of biofilms limits the spread of cheaters, but the long-term influence of cheating on biofilm evolution is not well understood. In addition, the influence of cheats on phenotypic heterogeneity pattern within matrix-producers, was never examined. Here, we describe the long-term dynamics between EPS producers (cooperators) and non-producers (cheaters) in *B. subtilis* biofilms and track changes in phenotypic heterogeneity of matrix production within the populations of co-operators. We discovered that cheater-mediated evolution in pellicles leads to a transient shift in phenotypic heterogeneity pattern of co-operators, namely an increased number of *eps* expressing cells as depicted by hyper ON phenotype. Although hyper ON strategy seems adaptive in presence of cheats, it is soon substituted by hyper OFF phenotype and/or soon after by population collapse. This study provides additional insights on how biofilms adapt and respond to stress caused by exploitation in long-term scenario.

SIGNIFICANCE STATEMENT

Microbial biofilms are significant in medical, environmental and industrial settings. Biofilm control strategies have been proven to be challenging due to their increased resistance to antimicrobials. Here, we employ a cheater-mediated evolution study in *Bacillus subtilis* pellicles to understand in long-term scale how biofilms' social behavior evolves as triggered by stress. We show that evolution of matrix-producing cells (cooperators) in the presence of non-producers

bioRxiv preprint doi: https://doi.org/10.1101/494716; this version posted December 13, 2018. The copyright holder for this preprint (which was not certified by peer review) is the author/funder, who has granted bioRxiv a license to display the preprint in perpetuity. It is made available under aCC-BY 4.0 International license.

(cheaters) leads to a cheating strategy that allows cheaters to benefit from cooperators, that subsequently result to population tragedy. However, cooperators can also adapt and evade exploitation via an anti-cheating system that involves shift in phenotypic heterogeneity related to biofilm matrix expression. This study highlights biofilm adaptation and stress response mechanisms within the context of evolution.

INTRODUCTION

Cooperative interactions are prevalent for all life forms (1), even for simple microbes that often exist in communities of matrix bound surface-attached cells called biofilms (2–6). However, when costly products such as siderophores (7, 8), extracellular polymeric substances (9, 10), digestive enzymes (11), and signaling molecules (12, 13) are secreted and shared, cooperative behavior becomes susceptible to cheating (2, 14–16), where mutants defective in cooperation can still benefit from cooperative community members (4, 5, 17). It has been shown that spatially structured biofilms, where interactions with clonemates are common and diffusion of public goods is limited, may serve as natural defense against cheating (18–20). However, long time scale studies have recently reported that biofilm defectors can spontaneously emerge and spread in biofilms by exploiting other matrix-proficient lineages (21–24). In fact, a pioneering microbial evolution study on *Pseudomonas fluorescens* has already pointed towards dynamic evolutionary interplay between cooperation and exploitation in biofilm matts (25), where emergence of cellulose overproducer (Wrinkly) allowed matt formation, but also created an opportunity for exploitation by non-producers (Smooth), eventually leading to so called 'tragedy of the commons' (4, 26, 27).

Taken together, biofilms are suitable model to understand social interactions in an evolutionary time scale (23, 28–31). Modelling and empirical data confirm that mutualism (beneficial to both actor and recipient) and altruism (beneficial to recipient but not to actor) play crucial role in biofilm enhancement (32) but at the same time can lead to biofilm destabilization (25). Can

bioRxiv preprint doi: https://doi.org/10.1101/494716; this version posted December 13, 2018. The copyright holder for this preprint (which was not certified by peer review) is the author/funder, who has granted bioRxiv a license to display the preprint in perpetuity. It is made available under aCC-BY 4.0 International license.

cooperators evolve tactics to evade exploitation and in turn, can cheats utilize evolution to enhance their selfish actions?

Recent studies showed that in well-mixed environment, cooperators adapt to cheats by reducing cooperation (14, 15, 33). Such reduction could be achieved by various strategies, for instance decrease in motility (15), down regulation or minimal production in public goods (14, 15, 33), up-regulation of other alternative public goods (14), or bi-stable expression in virulence gene (2). Interestingly, populations of cooperators often exhibit phenotypic heterogeneity at the single cell level (34, 35). Therefore, an alternative and simple mechanism to modulate levels of cooperation in a population, would be through changes in phenotypic heterogeneity pattern. However, the long-term effects of cheats on costly goods' expression at individual cell level have never been examined. Understanding how heterogeneity of gene expression within the population is affected in the presence of cheats would provide better insight on microbial adaptation and stress response mechanisms.

Here, we address this question using pellicle biofilm model of *Bacillus subtilis.* Pellicle formation in *B. subtilis* involves, amongst others, aerotaxis driven motility and subsequent matrix production (36). Aerotaxis is important for oxygen sensing to aid cells reach the surface, while matrix formation is significant to sustain cells to adhere to the surface and to each other. Exopolysaccharide (EPS) is a costly public good in *Bacillus subtilis* biofilms (10, 18, 37) and is heterogeneously expressed during biofilm formation with approximately 40% of cells exhibiting the ON state (37, 38). We aimed to investigate the long-term dynamics between EPS producer (cooperator) and EPS deficient (cheater) cells and assess cheat-dependent alteration related to phenotypic heterogeneity in *eps* expression by the producer.

We reveal, that initial cheating mitigation by the EPS producers involves shift in phenotypic heterogeneity towards increased frequency of *eps*-expressing cells, which is achieved by loss-of-function mutation in a single regulatory gene. We also demonstrate, that although 'hyper ON' phenotype helps to reduce cheating, it is rapidly replaced by hyper OFF strategy, which,

bioRxiv preprint doi: https://doi.org/10.1101/494716; this version posted December 13, 2018. The copyright holder for this preprint (which was not certified by peer review) is the author/funder, who has granted bioRxiv a license to display the preprint in perpetuity. It is made available under aCC-BY 4.0 International license.

combined with certain mutations in EPS deficient strain, results in tragedy of the commons and population collapse. Our study uncovers an alternative anti-cheating mechanism based on changes in phenotypic heterogeneity and highlights meandering trajectories prior cooperation collapse.

RESULTS

Long-term cheating in pellicle biofilms leads to population collapse

Exopolysaccharide EPS is one of the major components of *B. subtilis* biofilm matrix and mutants deficient in EPS production (Δ*eps*) are not able to form pellicle biofilms (*SI Appendix*, Fig. S1A and S1B). Since it was previously demonstrated that EPS can be shared (10, 18, 37), we predicted that Δ*eps* would be able to take advantage of EPS-producing wild type (WT) and incorporate into the pellicle biofilm. Indeed, when co-cultivated with the WT (at 1:1 initial ratio), the Δ*eps* became part of the pellicle with negative impact on WT productivity (*SI Appendix*, Fig. S1b). In addition, presence of the mutant resulted in decreased level of surface complexity as typical wrinkly structures were absent in the mixed pellicle (*SI Appendix*, Fig. S1a). These results reveal that the Δ*eps* serves as cheater in the pellicle biofilms by taking advantage of the EPS producer strain.

In order to examine long-term population dynamics in co-culture of EPS producers (wild type-WT) and cheats (Δ*eps*), we allowed 8 parallel pellicle populations of Δ*eps*+WT to evolve for 35 cycles (~200 generations) starting at 1:1 initial ratio. Every 5th transfer, we determined relative frequencies (%) of both strains in the pellicles using plate count assay (CFU/ml). The results revealed that cheats were able to outnumber the producer strain, eventually leading to decreased productivity of the entire population, as pellicle formation was no longer possible (Fig. 1). Such scenario was observed in 6 out of 8 populations and will be referred to as population collapse (Fig. 1). Evolutionary time points when a collapse occurred varied among the population, for instance in population 1 and 7, the collapse was observed after 30th transfer

bioRxiv preprint doi: https://doi.org/10.1101/494716; this version posted December 13, 2018. The copyright holder for this preprint (which was not certified by peer review) is the author/funder, who has granted bioRxiv a license to display the preprint in perpetuity. It is made available under aCC-BY 4.0 International license.

while in population 2 it took place already after 10th transfer. No collapse was observed for populations 5 and 8, where cheats coexisted with WT until the end of the evolution cycle (35th). We also observed different patterns of how productivity of the WT changed when evolved in the presence of cheats (Fig. 1). A "decline-collapse" trend was noticed for populations 2, 3 and 4, wherein the WT continuously declined and then proceeded to population collapse after 5th, 15th and 10th transfers, respectively. For populations 1, 6 and 7, we witnessed a "decline-recovery-collapse" pattern. Finally, we detected a "decline-recovery-no collapse" model for populations 5 and 8, wherein the populations after recovering from an early decline persisted until 35th transfer.

'Hyper ON' matrix producers emerge during evolution with cheats

Previous studies have shown that cooperators can adapt to presence of cheats for example by decreasing the amount of released public goods and therefore minimizing cheating opportunities (2, 14, 15). As *B. subtilis* exhibits phenotypic heterogeneity in *eps* matrix gene expression (37, 38) (*SI Appendix*, Fig. S2), we investigated how such heterogeneous expression is influenced by the presence of cheats in an evolutionary perspective. Using confocal laser scanning microscopy, qualitative assessment of randomly selected isolates revealed that early populations of the EPS producers (5-10 transfer) which co-evolved with cheats exhibited a so called hyper ON phenotype, where the fraction of *eps* expressing cells was largely increased as compared to the ancestral strain (*SI Appendix*, Fig. S2). On the contrary, evolution in the absence of Δ*eps* mostly resulted in hyper OFF phenotype, with larger amounts of cells that do not express *eps*. To further verify this phenomenon, we quantified the average P_{eps}-GFP intensity of 95 single isolates per each WT population (see methods) (Fig. 2). The results revealed major changes in distribution of P_{eps}-GFP intensity across the evolved and co-evolved WT populations as compared to the WT ancestor (Fig. 2). Specifically, for all WTs evolved alone, the distributions narrowed and dramatically shifted to the left, so that the clear majority of isolates matched the hyper OFF

bioRxiv preprint doi: https://doi.org/10.1101/494716; this version posted December 13, 2018. The copyright holder for this preprint (which was not certified by peer review) is the author/funder, who has granted bioRxiv a license to display the preprint in perpetuity. It is made available under aCC-BY 4.0 International license.

category across the entire evolutionary time (5-35th transfer) (Fig. 2.). On the contrary, in some co-evolved WT populations (population 3, 5 and 7) the distributions widened at the 10th transfer (Fig. 2), resulting in increased frequency of hyper ON isolates (Fig. 2). A transient increase of hyper ON phenotype frequency appeared rather temporary, as it was followed by dramatic increase in frequency of hyper OFF phenotype in later evolutionary time points (Fig. 2.).

Mutations in *rsiX* lead to Hyper ON phenotype

To unravel the genetic basis of the hyper ON phenotype that evolved in presence of cheats, several single isolates from the evolved populations were subjected to genome resequencing (for details see methods). The comparative analysis of sequencing data revealed that the WT isolates that co-evolved with cheats and exhibited the hyper ON phenotype, shared mutations in *rsiX* gene (*SI Appendix*, Dataset S1). The *rsiX* gene encodes for an anti-sigma factor that controls the activity of extracellular cytoplasmic function (ECF) sigma factor X which is involved in cationic antimicrobial peptide resistance important for cell envelope stress response (39). Detected mutations resulted either in substitution of Valine 106 to Alanine or frameshift mutations in Serine 104 or Isoleucine 347 that could lead to change or loss of anti-SigX function. Indeed, we were able to recreate the evolved hyper ON phenotype in the pellicle solely by deleting the *rsiX* gene in the WT ancestor (Fig. 3C). Interestingly, a different type of frameshift mutation in Lysine 200 was found in one population of evolved WT alone but this population demonstrated a hyper OFF phenotype (Fig. 3A), suggesting that only certain types of mutations in *rsiX* lead to the increase in number of *eps* expressing cells in the population or additional mutations have antagonistic effects in this isolate.

Mutation in *rsiX* contributes to competitive advantage of producer strains against cheats

As mutation in *rsiX* resulted in hyper ON phenotype that may be linked to elevated secretion of EPS, we hypothesized that Δ*rsiX* producers could support the spread of cheats and contribute to

bioRxiv preprint doi: https://doi.org/10.1101/494716; this version posted December 13, 2018. The copyright holder for this preprint (which was not certified by peer review) is the author/funder, who has granted bioRxiv a license to display the preprint in perpetuity. It is made available under aCC-BY 4.0 International license.

population collapse scenario (Fig.1). To better understand how ancestor WT and Δ*rsiX* interact with Δ*eps,* we cultivated the Δ*eps* in presence of EPS-containing supernatants obtained from the WT and Δ*rsiX* (*SI Appendix*, Fig. S4). Both supernatants could partially restore pellicle formation by Δ*eps* resulting in similar productivities of Δ*eps,* thereby not supporting our hypothesis on improved performance of the mutant in presence of hyper ON Δ*rsiX* strain.

In order to determine the effect of *rsiX* deletion on fitness of the WT in presence of cheats, we performed a series of competition assays. Apparently, the Δ*rsiX* showed two-fold increase in relative frequency (40%) (Fig. 4 and *SI Appendix*, Fig. S5) when competed against the Δ*eps*, as compared to the WT ancestor (20%).

It is worth to mention that we could not detect any significant fitness costs or benefits linked to *rsiX* deletion in pairwise competition between Δ*rsiX* and WT (*SI Appendix*, Fig. S5; relative fitness of Δ*rsiX* = 1.00 ±0.02 S.D.). Furthermore, we did not observe significant differences in productivities of WT and the hyper ON Δ*rsiX* mutant, when grown in monoculture pellicles (*SI Appendix*, Fig. S3), suggesting that positive effect of *rsiX* mutation only manifests in presence of cheats.

Relative frequencies of the evolved WT strains carrying hyper ON phenotype and specific mutations in *rsiX* were even higher (average ranged from 58% to 99%) as compared to Δ*rsiX* carrying ancestral genetic background (Fig. 4, Fig. S6). Remarkably, the significant fitness improvement of the WT evolved with cheats was already observed in 5th transfer and 10th transfer, mutually with an early occurrence of hyper ON phenotype in those populations. This was not the case for the WT evolved alone at 5th transfer (20%), where a remarkable fitness increase (average ranged from 87% to 94%) could only be observed in later evolutionary time point (Fig. 4 and *SI Appendix*, Fig. S6). These results suggest that the early improvement in competitive strategies against cheats are caused by the *rsiX* mutation and other mutations associated with hyper ON phenotype, while in later evolutionary time points this effect can be amplified by cheating-independent adaptation to the medium. Interestingly, frequencies of Δ*eps*

bioRxiv preprint doi: https://doi.org/10.1101/494716; this version posted December 13, 2018. The copyright holder for this preprint (which was not certified by peer review) is the author/funder, who has granted bioRxiv a license to display the preprint in perpetuity. It is made available under aCC-BY 4.0 International license.

in pellicles formed by the ancestor or evolved matrix producers, did not manifest in productivity assay (Fig. 4b). These suggests that hyper ON phenotypes are vested on the increase in *eps*-expressing cells or limiting the spread of cheats but do not result in an increase in total yield.

sinR mutation negatively affects the competitive advantage of cheats

Interestingly, evolved cheaters that were isolated from the same populations as *rsiX* mutation containing matrix producers (i.e. populations 3 at 5th and 10th transfers and 7 at 10th and 30th transfers), harbored a *sinR* mutation of an amino acid substitution from Leucine 1 to Tryptophan (*SI Appendix*, Dataset S1). Therefore, we anticipated that the mutation may influence competitive fitness of the Δ*eps* against the WT matrix producer. The *sinR* gene encodes for a transcriptional repressor and biofilm master regulator that controls the operons e*psA-O* and *tapA-sipW-tasA* for matrix exopolysaccharide and protein component, respectively (40). Interestingly, our results showed that the evolved Δ*eps* with an ancestor *sinR* (Δ*eps sinR*^{WT}) performed better against the WT ancestor as compared to evolved Δ*eps* that carried *sinR* mutation (Δ*eps sinR*^{Leu1Trp}) (Fig. 5 and *SI Appendix*, Fig. S7), suggesting that mutation in *sinR* could prevent the spread of cheats in the evolved populations, especially at early stage of co-evolution (Fig. 4 and *SI Appendix*, Fig. S6). Interestingly, the impact of *sinR* mutation in Δ*eps* is nearly lost when WT carries *rsiX* deletion or other adaptive mutations (Fig. 5 and *SI Appendix*, Fig. S7, S8).

Population collapse may be linked to adaptive mutations in cheats and loss of _rsiX_ mutants in producer populations

To explore possible reasons behind the collapse of certain WT vs Δ*eps* populations, the co-evolved populations of WTs and Δ*eps* were isolated from selected co-cultures stocks (see methods) at final evolutionary timepoint (populations 5 and 8) or at last time point prior to collapse (populations 4 and 6) and subjected to whole genome re-sequencing. Genomic analysis of Δ*eps* populations that caused early pellicle collapse (pop 4 and 6) revealed several mutations

bioRxiv preprint doi: https://doi.org/10.1101/494716; this version posted December 13, 2018. The copyright holder for this preprint (which was not certified by peer review) is the author/funder, who has granted bioRxiv a license to display the preprint in perpetuity. It is made available under aCC-BY 4.0 International license.

in chemo/aerotaxis genes, namely in *hemAT* (Fig. 6 and *SI Appendix*, Dataset S2) with amino acid change from Glutamic acid 254 to Lysine and Lysine 131 to Threonine for populations 6 and 4, respectively. Interestingly, we did not identify any genetic changes in WT from population 4, suggesting that the collapse was triggered by adaptation of the Δ*eps.* On the other hand, for the non-collapsed populations (population 5 and 8) the consensus could be observed in the WTs, which showed mutations in *yvrG* gene (Fig. 6 and *SI Appendix*, Dataset S2) encoding for two-component histidine kinase involved in cell wall process. Finally, *rsiX* mutation was not detected neither in the last populations before collapse, with an exemption of population 7 with 1% hyper ON phenotype (Fig. 2, 6 and *SI Appendix*, Dataset S1), nor at the last transfer point for the non-collapse, implying that this mutation was lost in parallel with the loss of hyper ON phenotype in the late populations.

DISCUSSION

Studies on evolution of cooperative behavior is important to understand how social behaviors are shaped in longer time scale. Moreover, exploring long term consequences of exposure to cheating allows to better understand how cooperation prevails in nature where environmental stress and exploitation exist inherently. Previous evolution studies on cheater-cooperator interactions in spatially structured environment showed cheater mitigation via minimization of the cooperative trait (2, 14, 15). On the contrary, here we show that cooperators initially respond to cheating by intensifying the cooperative behaviors through shift in phenotypic heterogeneity pattern towards hyper ON phenotype, where, in contrast to the ancestral strain, nearly all members of the population express the operon involved EPS production. Further molecular analysis of the hyper ON isolates strongly suggests that this phenotype is triggered by loss-of-function mutation in *rsiX* gene. The product of *rsiX* represses the activity of ECF sigma factor, SigX that is involved cell envelope stress response against cationic antimicrobial peptides (41). Importantly, SigX has been previously shown to induce expression of *epsA-O* in B. subtilis via a

bioRxiv preprint doi: https://doi.org/10.1101/494716; this version posted December 13, 2018. The copyright holder for this preprint (which was not certified by peer review) is the author/funder, who has granted bioRxiv a license to display the preprint in perpetuity. It is made available under aCC-BY 4.0 International license.

complex regulatory pathway involving Abh and SlrR (42), explaining the observed enhanced in *eps* gene expression in *rsiX* mutant. Another example of matrix overproduction via ECF adaptation was also reported in Gram-negative bacterium *Pseudomonas aeruginosa* where mutations in another ECF called AlgT led to alginate overproduction and increased resistance to antimicrobials (43). Therefore, adaptive boosts in matrix production through modulation of ECF is not exclusive for *B. subtilis* but seems to occur also in medically relevant Gram-negative pathogens like *P. aeruginosa*.

Interestingly, we also observed that *rsiX* mutation carrying matrix producers tend to co-occur with $sinR^{Leu1Trp}$ cheaters (Δ*eps*) (Fig. 6 *SI Appendix*, Dataset S1). SinR is a transcriptional repressor and master regulator of biofilm (40) and changes in the N terminal of SinR reveal big impact on its functions (44), we expect that alterations in the first amino acid could provide immense effect either on translation rate, folding stability or function. We have previously observed that loss-of-function mutation in Δ*eps* enhances the production of TasA, a protein constituent which is another essential matrix component (37). Furthermore, biofilm productivity can be maximized by division of labor between TasA- and EPS-producers (37). We hypothesize that similar phenomenon might transiently improve productivity of mixed pellicles, where cooperators overproduced EPS while cheaters overproduced TasA. Alternatively, as TasA carries antimicrobial properties (45, 46), its increased abundance could trigger stress response in the co-operator, selecting for *rsiX* mutation. This could explain the synchronous appearance of *rsiX* mutations with hyper ON phenotypes in evolved cooperators and *sinR* mutations in evolved cheaters.

In contrast to previous studies, that addressed long term cheating on diffusible siderophores, we explored evolutionary interplay between biofilm producers and non-producers in structured environment. Our results support previous observations on evolution of specific cheating-resisting mechanisms in co-operators, pointing towards ubiquity of this phenomenon. In addition, our work brings up two major findings 1) matrix producers can adapt to matrix non-producers by shifting phenotypic heterogeneity towards increased number of matrix-expressing

bioRxiv preprint doi: https://doi.org/10.1101/494716; this version posted December 13, 2018. The copyright holder for this preprint (which was not certified by peer review) is the author/funder, who has granted bioRxiv a license to display the preprint in perpetuity. It is made available under aCC-BY 4.0 International license.

cells 2) hyper ON anti-cheating strategy is a short-term solution, which can either be replaced by another, yet unknown strategy linked to hyper OFF phenotype, or followed by tragedy of the commons. As recently demonstrated, alternative EPS-independent biofilm formation strategies can emerge by single amino acid change is TasA (47). It remains to be discovered whether shifts in phenotypic heterogeneity in response to long term cheating is general phenomenon that applies to different types of public goods.

MATERIALS AND METHODS

Bacterial strains and culture conditions

Strain *B. subtilis* 168 $P_{hyperspank}$-mKATE P_{eps}-GFP (TB869) was obtained by transforming the laboratory strain, *B. subtilis* 168 $P_{hyperspank}$-mKATE (TB49) (10, 18), with genomic DNA from NRS2243 (*sacA*::P_{epsA}-*gfp*(Km)*hag*::cat) and selecting for Km resistance. The Δ*rsiX* strain with fluorescence reporters (TB959) was obtained by transforming TB869 with genomic DNA isolated from BKE23090 (168 *trpC*2 Δ*rsiX*::erm) (48). Strains were maintained in LB medium (Lysogeny Broth (Lennox), Carl Roth, Germany), while 2×SG medium was used for biofilm induction (10). The Δ*eps* strains (TB608) was created previously (10).

Experimental evolution

Eight biological replicates of the co-cultures of 1:1 ratio of *B. subtilis* TB869 and TB608 were grown in 48-well plate containing 1ml 2×SG medium at 30°C for two days. Pellicles were harvested into Eppendorf tubes containing 500 µl sterile 2×SG medium and 100 µl of sterile glass sand, vortexed for 90 seconds, 10 µl fraction was transferred into 1ml 2×SG medium of a 48 well plate, and incubated at 30°C static condition for two days. This cycle was continuously repeated 35 times. As control, four biological replicates of mono-cultures of *B. subtilis* TB869 were evolved using the same transfer method. Every 5th transfer cycle, harvested cultures were mixed with 15% glycerol and stored at –80°C.

bioRxiv preprint doi: https://doi.org/10.1101/494716; this version posted December 13, 2018. The copyright holder for this preprint (which was not certified by peer review) is the author/funder, who has granted bioRxiv a license to display the preprint in perpetuity. It is made available under aCC-BY 4.0 International license.

Population ratio assay

At every 5th transfer, pellicle biofilm productivities and relative frequencies of mutants and WT were qualitatively assessed (colony forming units (CFU)/ml) using LB agar containing selective antibiotics. LB agar plates were incubated at 37°C for 16 hours and colonies were counted. Three single clones of WT and of *Δeps* per population per timepoint were isolated from plates and stored at –80°C in the presence of 15% glycerol.

Quantitative assessment of hyper ON and hyper OFF populations

Ninety-five single isolates of ancestor or evolved TB869 strains obtained from the population per timepoint were allowed to form pellicles in 96-well PCR plate containing 100µl 2×SG medium. After incubation at 30°C for 24 hours, the plate was vortexed for 90 seconds, bath sonicated (mini ultrasonic bath, Carl Roth, Germany) for 5 minutes and fluorescence was recorded using TECAN Infinite F200 PRO microplate reader (excitation at 485/20 nm and emission at 535/10 nm for GFP; excitation at 590/20 nm and emission at 635/35 nm for RFP; using manual gain of 35 and 50 for GFP and RFP, respectively). Hyper ON and hyper OFF phenotypes were categorized based on cut off value of the WT ancestor mean ± 1SD. GFP intensity values above 134 arbitrary units (AU) were considered as hyper ON and values below 70 AU were categorized as hyper OFF.

Pellicle competition assay

Pellicles grown from 1:1 ratio of competing strains and incubated for two days were subjected to competition assay as previously described (10).

Qualitative assessment of Hyper ONs and Hyper OFFs via microscopy

Single clones of WT obtained from population ratio assay were allowed to form 1-day old pellicle. Harvested pellicles were subjected to microscopic analysis using an Axio Observer 780 Laser

bioRxiv preprint doi: https://doi.org/10.1101/494716; this version posted December 13, 2018. The copyright holder for this preprint (which was not certified by peer review) is the author/funder, who has granted bioRxiv a license to display the preprint in perpetuity. It is made available under aCC-BY 4.0 International license.

Scanning Confocal Microscope (Carl Zeiss) equipped with a Plan-Apochromat 63×/1.4 Oil DIC M27 objective, an argon laser for stimulation of fluorescence (excitation at 488 for green fluorescence and 561 nm for red fluorescence, with emission at 528/26 nm and 630/32 nm respectively). Zen 2012 Software (Carl Zeiss) and FIJI Image J Software (49) were used for image recording and processing, respectively.

Genome re-sequencing and genome analysis

Genomic DNA of single clones from selected evolved populations were isolated using Bacterial and Yeast Genomic DNA kit (EURx) directly from –80°C stocks grown in LB medium for 5 hours at 37°C with shaking at 220 rpm. For population sequencing analysis, approx. 100 colonies belonging to the evolved populations were harvested into 2ml LB broth and incubated at 37°C shaking at 220 rpm for 2-3 hours. Re-sequencing was performed on an Illumina NextSeq instrument using V2 sequencing chemistry (2x150 nt). Base-calling was carried out with "bcl2fastq" software (v.2.17.1.14, Illumina). Paired-end reads were further analyzed in CLC Genomics Workbench Tool 9.5.1. Reads were quality-trimmed using an error probability of 0.05 (Q13) as the threshold. Reads that displayed ≥80% similarity to the reference over ≥80% of their read lengths were used in mapping. Quality-based SNP and small In/Del variant calling was carried out requiring ≥10× read coverage with ≥25% variant frequency. Only variants supported by good quality bases (Q ≥ 30) on both strands were considered. Gene functions (product names) in *SI Appendix* Datasets were reported based on SubtiWiki (50).

Acknowledgements

This work was funded by the Deutsche Forschungsgemeinschaft (DFG) to Á.T.K. (KO4741/2.1) within the Priority Program SPP1617. M.M. was supported a FEMS Research and Training Grant (FEMS-RG-2017-0054). A.D. has received funding from the European Union's Horizon 2020 research and innovation programme under the Marie Sklodowska-Curie grant agreement no.

bioRxiv preprint doi: https://doi.org/10.1101/494716; this version posted December 13, 2018. The copyright holder for this preprint (which was not certified by peer review) is the author/funder, who has granted bioRxiv a license to display the preprint in perpetuity. It is made available under aCC-BY 4.0 International license.

713683 (H.C. Ørsted COFUND). Work in the laboratory of Á.T.K. is supported by a DTU startup fund and partly by the Danish National Research Foundation (DNRF137) for the Center for Microbial Secondary Metabolites.

Authors contributions

Á.T.K. conceived the project, M.M., A.D., and D.S. performed the experiments. G.M contributed with methods. M.M., A.D. and Á.T.K. wrote the manuscript, with all authors contributing to the final version.

bioRxiv preprint doi: https://doi.org/10.1101/494716; this version posted December 13, 2018. The copyright holder for this preprint (which was not certified by peer review) is the author/funder, who has granted bioRxiv a license to display the preprint in perpetuity. It is made available under aCC-BY 4.0 International license.

REFERENCES

1. Bourke A (2011) *Principals of social evolution: Oxford series in ecology and evolution.* (Oxford University Press, Oxford, UK).
2. Diard M, et al. (2013) Stabilization of cooperative virulence by the expression of an avirulent phenotype. *Nature* 494:353–356.
3. Nadell CD, Xavier JB, Foster KR (2009) The sociobiology of biofilms. *FEMS Microbiol Rev* 33:206–224.
4. West SA, Diggle SP, Buckling A, Gardner A, Griffin AS (2007) The social lives of microbes. *Annu Rev Ecol Evol Syst* 38:53–77.
5. West S a., Griffin AS, Gardner A (2007) Evolutionary explanations for cooperation. *Curr Biol* 17:661–672.
6. Xavier J, Foster KR (2007) Cooperation and conflict in microbial biofilms. *Proc Natl Adac Sci USA* 104:876–881.
7. Luján AM, Gómez P, Buckling A (2015) Siderophore cooperation of the bacterium Pseudomonas fluorescens in soil. *Biol Lett* 11:20140934.
8. Weigert M, Kümmerli R (2017) The physical boundaries of public goods cooperation between surface-attached bacterial cells. *Proc R Soc B Biol Sci* 284:20170631.
9. Dragoš A, Kovács ÁT (2017) The peculiar functions of the bacterial extracellular matrix. *Trends Microbiol* 25:257–266.
10. Martin M, et al. (2017) *De novo* evolved interference competition promotes the spread of biofilm defectors. *Nat Commun* 8:15127.
11. Folse HJ, Allison SD (2012) Cooperation, competition, and coalitions in enzyme-producing microbes: Social evolution and nutrient depolymerization rates. *Front Microbiol* 3:338.
12. Popat R, et al. (2012) Quorum-sensing and cheating in bacterial biofilms. *Proc R Soc B Biol Sci* 279:4765–4771.

bioRxiv preprint doi: https://doi.org/10.1101/494716; this version posted December 13, 2018. The copyright holder for this preprint (which was not certified by peer review) is the author/funder, who has granted bioRxiv a license to display the preprint in perpetuity. It is made available under aCC-BY 4.0 International license.

13. Dogsa I, Oslizlo A, Stefanic P, Mandic-mulec I (2014) Social interactions and biofilm formation in *Bacillus subtilis*. *Food Technol Biotechnol* 52:149–157.

14. O'Brien S, Luján AM, Paterson S, Cant MA, Buckling A (2017) Adaptation to public goods cheats in *Pseudomonas aeruginosa*. *Proc R Soc B Biol Sci* 284:20171089.

15. Kümmerli R, et al. (2015) Co-evolutionary dynamics between public good producers and cheats in the bacterium *Pseudomonas aeruginosa*. *J Evol Biol* 28:2264–2274.

16. Harrison F (2013) Dynamic social behaviour in a bacterium: *Pseudomonas aeruginosa* partially compensates for siderophore loss to cheats. *J Evol Biol* 26:1370–1378.

17. Hamilton WD (1964) The genetical evolution of social behaviour. I. *J Theor Biol* 7(1):1–16.

18. van Gestel J, Weissing FJ, Kuipers OP, Kovács ÁT (2014) Density of founder cells affects spatial pattern formation and cooperation in Bacillus subtilis biofilms. *ISME J* 8:2069–2079.

19. Nadell CD, Foster KR, Xavier JB (2010) Emergence of spatial structure in cell groups and the evolution of cooperation. *PLoS Comput Biol* 6:e1000716.

20. Momeni B, Waite AJ, Shou W (2013) Spatial self-organization favors heterotypic cooperation over cheating. *Elife* 2:e00960.

21. Dragoš A, et al. (2018) Evolution of exploitative interactions during diversification in *Bacillus subtilis* biofilms. *FEMS Microbiol Ecol* 94:fix155.

22. Ellis CN, Traverse CC, Mayo-Smith L, Buskirk SW, Cooper VS (2015) Character displacement and the evolution of niche complementarity in a model biofilm community. *Evolution (N Y)* 69:283–293.

23. Poltak SR, Cooper VS (2011) Ecological succession in long-term experimentally evolved biofilms produces synergistic communities. *ISME J* 5:369–378.

24. Goymer P, et al. (2006) Adaptive divergence in experimental populations of Pseudomonas fluorescens. II. Role of the GGDEF regulator WspR in evolution and development of the wrinkly spreader phenotype. *Genetics* 173:515–526.

bioRxiv preprint doi: https://doi.org/10.1101/494716; this version posted December 13, 2018. The copyright holder for this preprint (which was not certified by peer review) is the author/funder, who has granted bioRxiv a license to display the preprint in perpetuity. It is made available under aCC-BY 4.0 International license.

25. Rainey PB, Rainey K (2003) Evolution of cooperation and conflict in experimental bacterial populations. *Nature* 425:72–74.

26. West SA, Griffin AS, Gardner A, Diggle SP (2006) Social evolution theory for microorganisms. *Nat Rev Microbiol* 4:597–607.

27. Hardin G (1968) The tragedy of the commons. *Science (80-)* 162(June):1243–1248.

28. Martin M, Hölscher T, Dragoš A, Cooper VS, Kovács ÁT (2016) Laboratory evolution of microbial interactions in bacterial biofilms. *J Bacteriol* 198:2564–2571.

29. Traverse CC, Mayo-Smith LM, Poltak SR, Cooper VS (2013) Tangled bank of experimentally evolved *Burkholderia* biofilms reflects selection during chronic infections. *Proc Natl Acad Sci U S A* 110:E250-9.

30. Madsen JS, et al. (2015) Facultative control of matrix production optimizes competitive fitness in *Pseudomonas aeruginosa* PA14 biofilm models. *Appl Environ Microbiol* 81:8414–8426.

31. Rainey PB, Travisano M (1998) Adaptive radiation in a heterogeneous environment. *Nature* 394:69–72.

32. Kreft JU (2004) Biofilms promote altruism. *Microbiology* 150:2751–2760.

33. Lyons NA, Kolter R (2018) A single mutation in rapP induces cheating to prevent cheating in Bacillus subtilis by minimizing public good production. *Commun Biol* 1:133.

34. Veening JW, et al. (2008) Transient heterogeneity in extracellular protease production by *Bacillus subtilis*. *Mol Syst Biol* 4:1–15.

35. Davidson FA, Seon-Yi C, Stanley-Wall NR (2012) Selective heterogeneity in exoprotease production by *Bacillus subtilis*. *PLoS One* 7:e38574.

36. Hölscher T, et al. (2015) Motility, chemotaxis and aerotaxis contribute to competitiveness during bacterial pellicle biofilm development. *J Mol Biol* 427:3695–3708.

37. Dragoš A, et al. (2018) Division of labor during biofilm matrix production. *Curr Biol*

bioRxiv preprint doi: https://doi.org/10.1101/494716; this version posted December 13, 2018. The copyright holder for this preprint (which was not certified by peer review) is the author/funder, who has granted bioRxiv a license to display the preprint in perpetuity. It is made available under aCC-BY 4.0 International license.

28:1903–1913.

38. Chai Y, Chu F, Kolter R, Losick R (2008) Bistability and biofilm Formation in *Bacillus subtilis*. *Mol Microbiol* 67:254–263.

39. Helmann JD (2016) *Bacillus subtilis* extracytoplasmic function (ECF) sigma factors and defense of the cell envelope. *Curr Opin Microbiol* 30:122–132.

40. Chu F, et al. (2004) A master regulator for biofilm formation by Bacillus subtilis. *Mol Microbiol* 55(3):739–749.

41. Cao M, Helmann JD (2004) The *Bacillus subtilis* extracytoplasmic-function σX factor regulates modification of the cell envelope and resistance to cationic antimicrobial peptides. *J Bacteriol* 186(4):1136–1146.

42. Murray EJ, Strauch M a, Stanley-Wall NR (2009) SigmaX is involved in controlling *Bacillus subtilis* biofilm architecture through the AbrB homologue Abh. *J Bacteriol* 191:6822–6832.

43. Hentzer M, et al. (2001) Alginate overproduction affects Pseudomonas aeruginosa biofilm structure and function. *J Bacteriol* 183(18):5395–401.

44. Subramaniam AR, et al. (2013) A serine sensor for multicellularity in a bacterium. *Elife* 2013:1–17.

45. Stöver AG, Driks A (1999) Secretion, localization, and antibacterial activity of TasA, a *Bacillus subtilis* spore-associated protein. *J Bacteriol* 181:1664–1672.

46. Dragoš A, Kovács ÁT, Claessen D (2017) The role of functional amyloids in multicellular growth and development of Gram-positive bacteria. *Biomolecules* 7:60.

47. Dragoš A, et al. (2018) Collapse of genetic division of labour and evolution of autonomy in pellicle biofilms. 3:1451–1460.

48. Koo BM, et al. (2017) Construction and analysis of two genome-scale deletion libraries for *Bacillus subtilis*. *Cell Syst* 4:291–305.e7.

49. Rueden CT, et al. (2017) ImageJ2: ImageJ for the next generation of scientific image data.

bioRxiv preprint doi: https://doi.org/10.1101/494716; this version posted December 13, 2018. The copyright holder for this preprint (which was not certified by peer review) is the author/funder, who has granted bioRxiv a license to display the preprint in perpetuity. It is made available under aCC-BY 4.0 International license.

BMC Bioinformatics 18:529.

50. Zhu B, Stülke J (2018) SubtiWiki in 2018: From genes and proteins to functional network annotation of the model organism *Bacillus subtilis*. *Nucleic Acids Res* 46:D743–D748.

bioRxiv preprint doi: https://doi.org/10.1101/494716; this version posted December 13, 2018. The copyright holder for this preprint (which was not certified by peer review) is the author/funder, who has granted bioRxiv a license to display the preprint in perpetuity. It is made available under aCC-BY 4.0 International license.

Figure legends

Fig. 1. Population dynamics over the course of experimental evolution for eight parallel pellicle populations. Productivity (total CFU/ml) and cheater frequency (%) in the pellicle obtained from plate count assay (CFU/ml) for every 5th transfer starting from the initial count prior to incubation until 35 transfers.

Fig. 2. Quantitative assessment of hyper ONs and hyper OFFs present per evolved population. Percentage of isolates >134 AU value expressing high intensity level of P_{eps}-GFP (hyper ON) and low intensity value of < 70 AU (hyper OFF) for WT evolved and non-evolved strains per timepoint from 5th to 35th transfer for all 8 populations evolved with cheaters and 4 populations evolved alone (n=95). Cut off based on the mean ± 1SD of WT ancestor strain taken at six different days (n=336).

Fig. 3. Qualitative assessment of *eps* gene expression based on confocal laser scanning microscopy showing Δ*rsiX* phenotype similar to strains that were co-evolved with cheaters. Pellicles formed by single clones of evolved or *rsiX* mutated TB869 belonging to (A) population C1 evolved alone at 5th, 30th and 35th timepoint showing Hyper OFF phenotype (B) WT ancestor demonstrating heterogeneous expression (C) Δ*rsiX* exhibiting hyper ON phenotype similar to (D) evolved with cheaters Pop 3 (5th and 10th) and Pop 7 (30th) viewed under the confocal laser scanning microscope. Cells constitutively expressing mKATE are represented in magenta and *eps*-expressing cells are shown in green. Scale bar represents 10µm.

Fig. 4. (A) Pellicle competition assay of single clones belonging to producer populations (non-evolved (n=9), Δ*rsiX* (n=8), evolved with (n=4) and without cheaters (n=4)) against Δ*eps* ancestor and (B) corresponding pellicle productivity based on total CFU/ml. Mean is represented in square inside the box plots; whiskers represent the minimum and maximum; single dots represent the

bioRxiv preprint doi: https://doi.org/10.1101/494716; this version posted December 13, 2018. The copyright holder for this preprint (which was not certified by peer review) is the author/funder, who has granted bioRxiv a license to display the preprint in perpetuity. It is made available under aCC-BY 4.0 International license.

individual data points (n); asterisk (*) represents the significant difference from the WT ancestor ANOVA (P value 0.05).

Fig. 5. Pellicle competition assay against evolved cheater with *sinR*^{WT} (left) and *sinR*^{Leu1Trp} (right) (n=4) on single clones of producers (non-evolved, evolved with and without cheaters). Mean is represented in square; whiskers represent the minimum and maximum; single dots represent the individual data points (n); asterisk (*) represents the significant difference ANOVA (P value 0.05).

Fig. 6. Figure summary showing the population dynamics based on producer and cheater frequency per population from 5th transfer to 35th transfers for populations evolved with cheaters with collapse (Pop 1, 2, 3, 4, 6 and 7), without collapse (Pop 5 and 8), and populations evolved without cheaters (C1, C2, C3, C4) with indications of phenotypes based on hyper ON, hyper OFF or heterogenous *eps*-expression. Key mutations on single clone level of evolved WT and evolved Δ*eps* or population level are specified. *rsiX** mutation is not similar to mutation observed in strains evolved with cheaters.

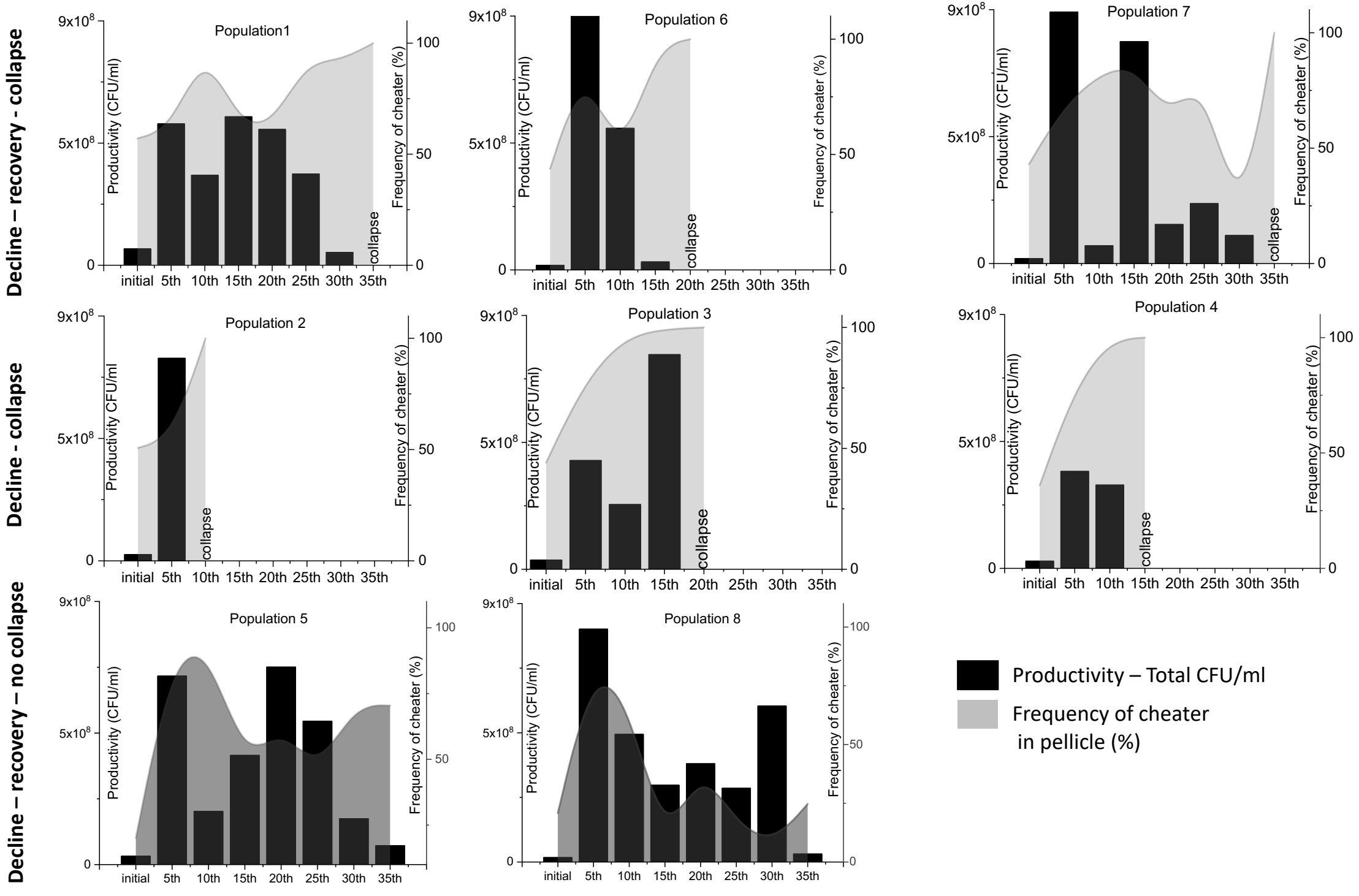
Decline – recovery - collapse
Decline - collapse
Decline – recovery – no collapse
Population1
Population 6
Population 7
Population 2
Population 3
Population 4
Population 5
Population 8
Productivity (CFU/ml)
Productivity CFU/ml
Frequency of cheater (%)
collapse
9x10^8
5x10^8
0
100
50
initial 5th 10th 15th 20th 25th 30th 35th
Productivity – Total CFU/ml
Frequency of cheater in pellicle (%)

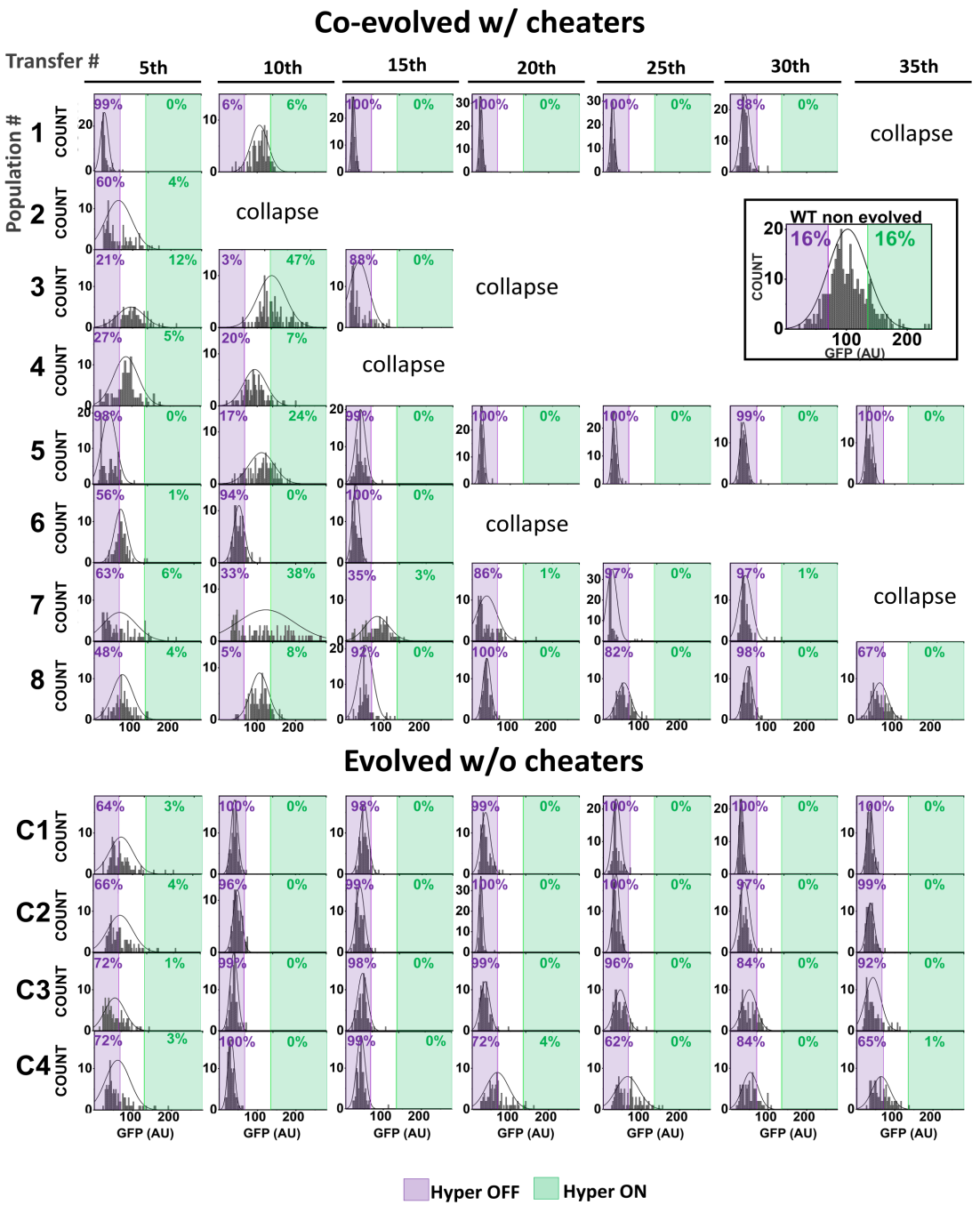
Co-evolved w/ cheaters
Transfer #
5th
10th
15th
20th
25th
30th
35th
Population #
1
2
3
4
5
6
7
8
COUNT
collapse
WT non evolved
16%
16%
GFP (AU)
Evolved w/o cheaters
C1
C2
C3
C4
Hyper OFF
Hyper ON

GFP
mKATE
Overlay
A)
Evolved w/o cheaters
5th C1
30th C1
35th C1
B)
WT ancestor
C)
ΔrsiX
D)
Evolved w/ cheaters
5th Pop 3
10th Pop 3
30th Pop 7

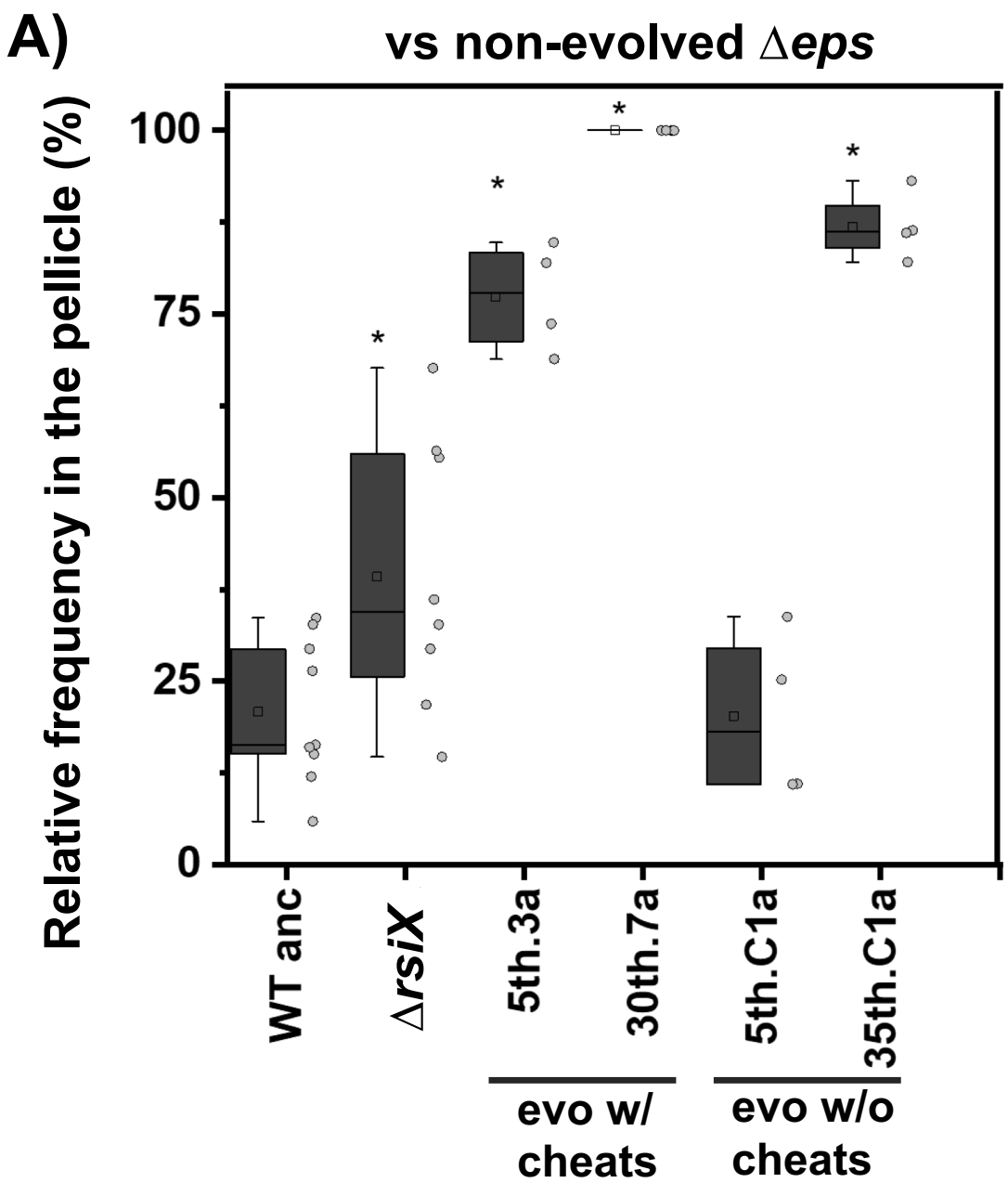
A)
vs non-evolved Δeps
Relative frequency in the pellicle (%)
100
75
50
25
0
*
*
*
*
WT anc
ΔrsiX
5th.3a
30th.7a
5th.C1a
35th.C1a
evo w/ cheats
evo w/o cheats

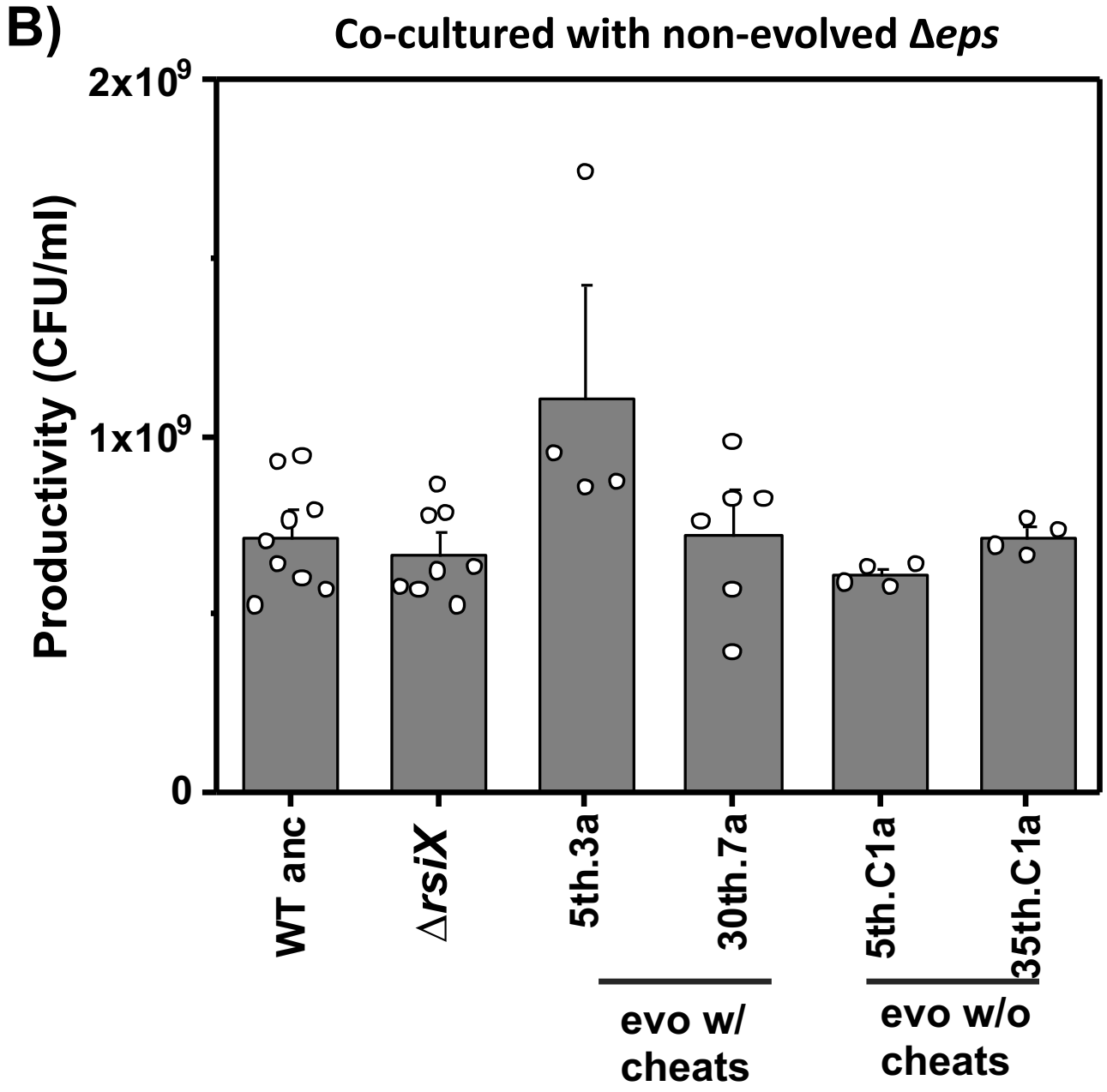
B)
Co-cultured with non-evolved Δeps
Productivity (CFU/ml)
2x10^9
1x10^9
0
WT anc
ΔrsiX
5th.3a
30th.7a
5th.C1a
35th.C1a
evo w/ cheats
evo w/o cheats

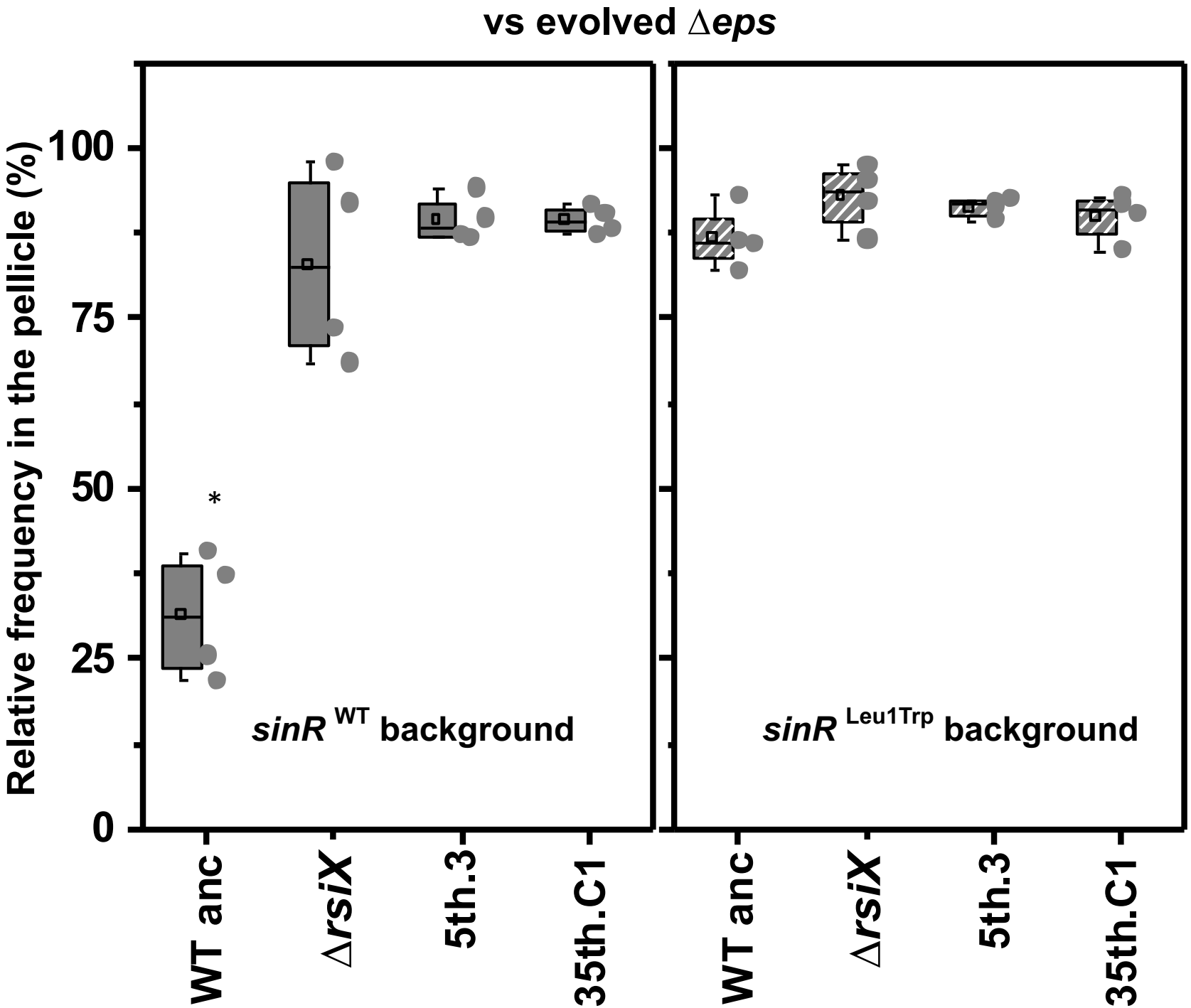
vs evolved Δeps
Relative frequency in the pellicle (%)
100
75
50
25
0
*
sinR WT background
sinR Leu1Trp background
WT anc
ΔrsiX
5th.3
35th.C1
WT anc
ΔrsiX
5th.3
35th.C1

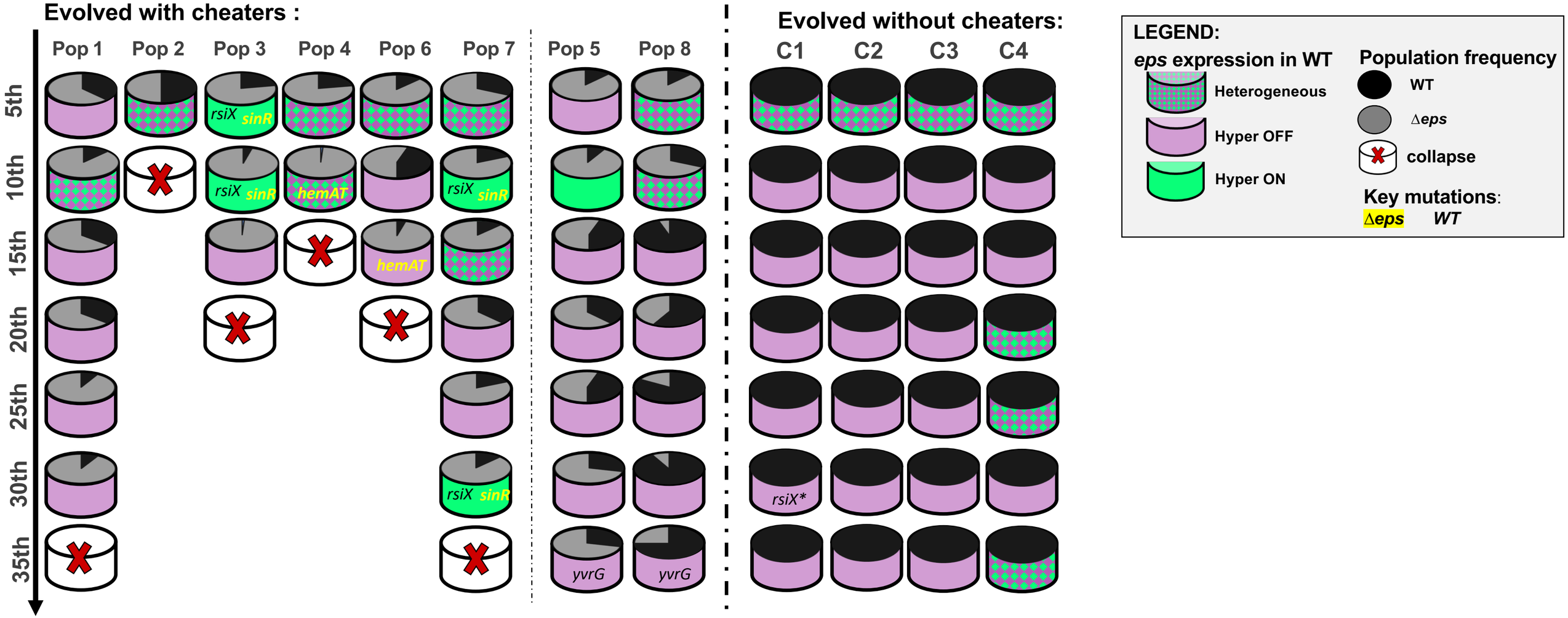
Evolved with cheaters :
Pop 1
Pop 2
Pop 3
Pop 4
Pop 6
Pop 7
Pop 5
Pop 8
5th
10th
15th
20th
25th
30th
35th
rsiX sinR
rsiX sinR
hemAT
rsiX sinR
hemAT
rsiX sinR
yvrG
yvrG
Evolved without cheaters:
C1
C2
C3
C4
rsiX*
LEGEND:
eps expression in WT
Heterogeneous
Hyper OFF
Hyper ON
Population frequency
WT
Δeps
collapse
Key mutations:
Δeps
WT